J Appl Phycol (2016) 28:897–905
DOI 10.1007/s10811-015-0617-2

Enhancing LC-PUFA production in *Thalassiosira pseudonana* by overexpressing the endogenous fatty acid elongase genes

Orna Cook[1] · **Mark Hildebrand**[1]

Received: 25 February 2015 / Accepted: 5 May 2015 / Published online: 17 May 2015

Abstract The health beneficial omega-3 long-chain polyunsaturated fatty acids (LC-PUFAs), eicosapentaenoic acid (EPA), and docosahexaenoic acid (DHA) are naturally synthesized by diatoms through consecutive steps of fatty acid elongase and desaturase enzymes. In *Thalassiosira pseudonana*, these fatty acids constitute about 10–20 % of the total fatty acids, with EPA accumulation being five to ten times higher than DHA. In order to identify the subcellular localization of enzymes in the pathway of LC-PUFA biosynthesis in *T. pseudonana* and to manipulate the production of EPA and DHA, we generated constructs for overexpressing each of the *T. pseudonana* long-chain fatty acid elongase genes. Full-length proteins were fused to GFP, and transgenic lines were generated. In addition, overexpressed native proteins with no GFP fusion were tested. The subcellular localization of each elongase protein was determined. We then examined the total amount of lipids and analyzed the fatty acid profile in each of the transgenic lines compared to wild type. Lines with overexpressed elongases showed an increase of up to 1.4-fold in EPA and up to 4.5-fold in DHA, and the type of fatty acid that was increased (EPA vs. DHA) depended on the type of elongase that was overexpressed. This data informs future metabolic engineering approaches to further improve EPA and DHA content in diatoms.

Keywords Omega-3 long-chain polyunsaturated fatty acids · Elongase · *Thalassiosira pseudonana* · Metabolic engineering

✉ Mark Hildebrand
mhildebrand@ucsd.edu

[1] Marine Biology Research Division, Scripps Institution of Oceanography, University of California, San Diego (UCSD), 9500 Gilman Dr., La Jolla, CA 92093-0202, USA

Introduction

Numerous studies in human health show that the omega-3 (n-3) long-chain polyunsaturated fatty acids (LC-PUFAs), eicosapentaenoic acid (EPA), and docosahexaenoic acid (DHA) play fundamental roles in the development and function of the human body (reviewed in Ruxton et al. 2004; Turchini et al. 2012; Kitessa et al. 2014). Among their various roles, n-3 LC-PUFAs are essential to neurodevelopment in infants and children and affect brain development and function (Rombaldi Bernardi et al. 2012) and visual and cognitive development during the first year of life (Molloy et al. 2012) and have beneficial effects in treating depression, ADHD, and Alzheimer's disease and reducing violence (Sinn et al. 2010), as well as in prevention and treatment of chronic diseases such as coronary heart disease, elevated triglyceride levels, cancer, and asthma (Simopoulos 2008). DHA in particular is found abundantly in the brain tissue (Soederberg et al. 1991), and application of DHA improves brain function in healthy and diseased mammals (Gamoh et al. 1999; Hashimoto et al. 2008).

Animal cells contain a pathway for synthesizing n-3 LC-PUFA using the essential fatty acid alpha-linolenic acid (ALA, 18:3n-3) as the precursor. However, the ability to convert ALA to EPA and DHA in mammals is very limited. Most of consumed ALA goes towards β-oxidation for either energy production (Leyton et al. 1987; Vermunt et al. 2000) or use in acetyl CoA for synthesis of saturated and mono-unsaturated fatty acid (FA) and cholesterol (Cunnane et al. 1999), whereas only a minor portion is utilized for the synthesis of EPA and DHA (Turchini et al. 2012). Since the amount produced in humans is below the requirement for healthy development and functioning, supplementary n-3 LC-PUFAs need to be consumed in the diet (Brenna et al. 2009). The main source of n-3 FA for human consumption is fish oil (Turchini et al.

2012). However, fish do not produce high amounts of these FAs but obtain them in their diet from the primary producers of n-3 PUFA which are microalgae (Harel et al. 2002; Atalah et al. 2007; Khozin-Goldberg et al. 2011; Turchini et al. 2012).

Biosynthesis of the n-3 LC-PUFAs EPA and DHA in eukaryotic cells including animals, plants, and microalgae takes place via the conventional pathway which involves consecutive steps of desaturation and elongation of the initial FA substrate, catalyzed by a set of fatty acid desaturases and fatty acid elongases (Wallis et al. 2002; Venegas-Calerón et al. 2010; Fig. 1). In photosynthetic organisms, i.e., plants and algae, the pathway starts with the product of de novo fatty acid synthesis, saturated C16 palmitic acid or saturated C18 stearic acid, while animal cells require the essential fatty acid α-linolenic acid (ALA) as the precursor of the pathway (Fig. 1). There are several ways to generate the final products EPA and DHA, and the particular steps to synthesize these n-3 FAs depend on the elongases and desaturases present in the cell (Fig. 1). Most animals including mammals do not have the delta 4-desaturase; therefore, in order to convert EPA to DHA, two steps of elongation are employed to generate C24:5 followed by the reaction of delta 6- desaturase to generate C24:6 which then converts to DHA (C22:6) through a beta-oxidation (Fig. 1; Voss et al. 1991). Organisms such as the microalgae *Euglena gracilis* or *Isochrysis galbana* contain genes that encode for delta 9-elongase and delta 8-desaturase and therefore use the alternative pathway in which elo9 elongates ALA to generate a C20:3 chain and then des8 adds the double bond to make C20:4 (Fig. 1 and Li et al. 2011; Qi et al. 2002; Wallis and Browse 1999).

Various types of microalgae, including diatoms, naturally synthesize a relatively high amount of the n-3 FAs. *Phaeodactylum tricornutum* accumulates up to 30 % of its lipids as EPA, but accumulates very little DHA (Grima et al. 1996), which is a desirable form for brain function (Gamoh et al. 1999; Hashimoto et al. 2002). *Thalassiosira pseudonana* contains up to 26 % of lipids of its dry weight, while 15–20 % of the lipids are the n-3 fatty acids EPA and DHA (Volkman et al. 1989; Tonon et al. 2002). *T. pseudonana* has a greater proportion of DHA than *P. tricornutum*, with a ratio of EPA/DHA of 3.6–3.7:1 for the former and 9.6–11.6:1 for the latter (Tonon et al. 2002). FA composition is commonly reported as percent of total lipid, which does not necessarily reflect the actual amount in a cell. For example, even though *P. tricornutum* is reported to have a higher percentage of EPA than *T. pseudonana*, on a per cell basis, it is lower, 275–425 fg cell^{-1} for *P. tricornutum* and 300–575 fg cell^{-1} in *T. pseudonana* (Tonon et al. 2002). *T. pseudonana*, like other photosynthetic eukaryotes, synthesizes n-3 FAs via the conventional pathway using elongases and desaturases to convert the saturated C16 fatty acid to EPA and DHA (Meyer et al. 2004; Tonon et al. 2004, 2005).

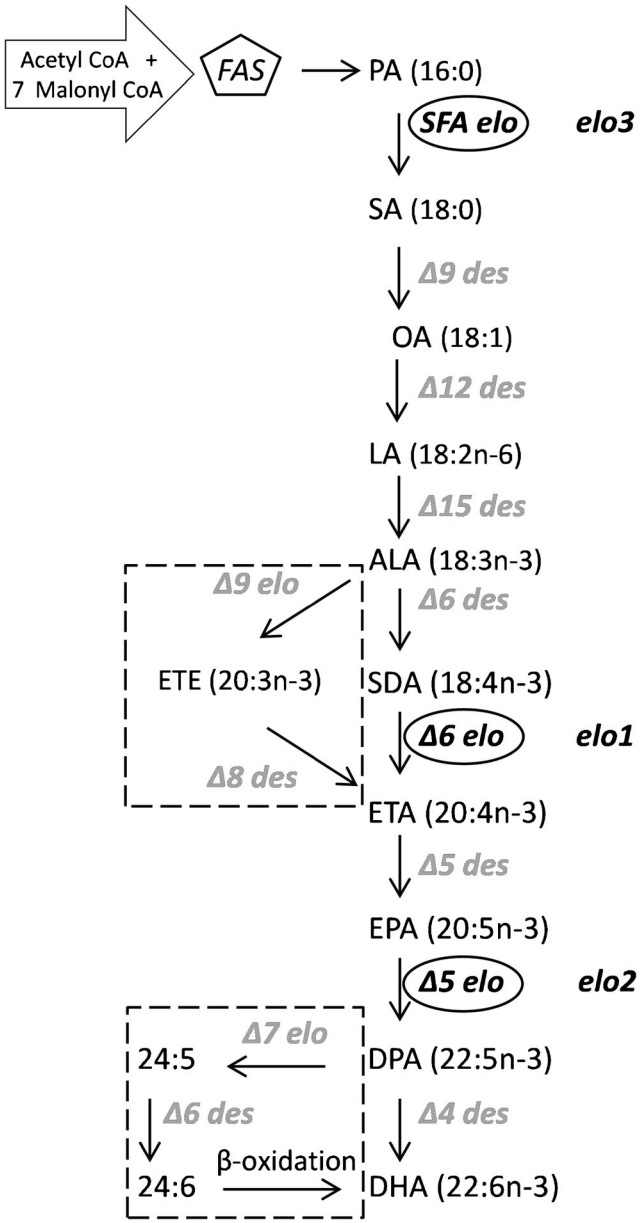

Fig. 1 Pathway of n-3 LC-PUFA biosynthesis in eukaryotic cells. *Boxed areas* denote steps that are absent in *T. pseudonana*. *Circled enzymes* are the three elongases characterized in this study. *PA* palmitic acid, *SA* stearic acid, *OA* oleic acid, *LA* linoleic acid, *ALA* α-linolenic acid, *SDA* stearidonic acid, *ETE* eicosatrienoic acid, *ETA* eicosatetraenoic acid, *EPA* eicosapentaenoic acid, *DPA* docosapentaenoic acid, *DHA* docosahexaenoic acid, *FAS* fatty acid synthase, *SFA* saturated fatty acid, *elo* elongase, *des* desaturase

In this study, we generated *T. pseudonana* lines that overexpress each one of the three endogenous elongase genes to determine their intracellular location and to evaluate the effect on EPA and DHA accumulation. The fatty acid composition in each of the elo overexpressing lines was analyzed in order to test their ability to increase production of LC-PUFA. The results clarified the role of the three elongases and improved accumulation of EPA and, more substantially, DHA.

Materials and methods

Thalassiosira pseudonana (CCMP1335) was grown with shaking or stirring and aeration, at 20 °C, under constant light condition in artificial sea water (ASW) medium (Darley and Volcani 1969) supplied with biotin and vitamin B_{12} at 1 μg L^{-1}. For Si starvation, cultures at exponential phase (~8×10^5 cells•mL^{-1}) were harvested; cells were washed with ASW without Si and re-suspended in the original volume of ASW without Si. Cells were maintained under starvation conditions at 20 °C under constant light for 24 h.

Plasmid construction and transformation The MultiSite Gateway® Technology was applied to generate vectors with the coding region of each one of the *T. pseudonana* elongase genes fused to the 5′ and 3′ flanking regions of the *T. pseudonana fcp* gene (Poulsen et al. 2006). Genomic DNA was extracted from wild-type *T. pseudonana* (Shrestha and Hildebrand 2015) and each of the three elongase genes was amplified by PCR with primers containing *att*B Gateway arms. The following sets of constructs were generated: fcpElo1 (Thaps3_3741), fcpElo1GFP, fcpElo2 (Thaps3_93), fcpElo2GFP and fcpElo3 (Thaps3_728), and fcpElo3GFP. PCR products were cloned into the gateway pDONOR vector using the Gateway BP clonase. Products were sequenced and were cloned into destination vectors pMHL78 and pMHL79 using the Gateway LR clonase to generate fcpElo or fcpEloGFP, respectively.

Transformation of *T. pseudonana* was done using microparticle bombardment with a Bio-Rad PDS-1000/He system (Dunahay et al. 1995). The presence of the constructs in the transformed lines was verified by PCR.

Fluorescence microscopy Subcellular localization of EloGFP proteins was visualized using a Zeiss Axio Observer fluorescence microscope. The GFP filter set was Zeiss #38HE (Ex 470/40 nm, FT 495, Em 525/50 nm), and chlorophyll was imaged using filter set no. 05 (Ex 395–440 nm, FT 460 nm, Em 470 nm LP).

Lipid analysis For lipid analysis, cultures were harvested at exponential phase (~8×10^5 cells•mL^{-1}), stationary phase (~6×10^6 cells•mL^{-1}), or 24 h Si starvation as described. Cells were washed with 0.4 M ammonium formate, centrifuged, and the pellets were kept in sealed tubes under N_2 at −80 °C until analysis. For quantitative lipid analysis, cells were lyophilized and their dry weight was determined. The pellet was resuspended in 1 M methanolic acid and incubated at 70 °C for 30 min for transesterification. Fatty acid methyl esters

```
Elo1  ----MDAYNAAMDKIGAAIIDWSDP---------------DGKFRADREDWWLCDFRSAI 41
Elo2  ----MCSPPPSQSKTTSLLARYTAAALLLLTL----TTWCHFAFPAATSTPGLTAEMHSY 52
Elo3  MSQFLTSIPKECVGTNGLGVHYAEFSCLHPLLGATYLPFERFYDPVATLTWMQDRPMIPI 60
          : :         .    ::                          .           .

Elo1  TIALIYIAFVILGSAVMQSLP---AMDPYPIKFLYNVSQIFLCAYMTVEAGFLAYRNGYT 98
Elo2  KVPLGLTVFYLLSLPSLKYVTDNYLAKKYDMKSLLTESMVLYNVAQVLLNGWTVYAIVDA 112
Elo3  IACVAYVVLIVLGRAYMKDRP---AWSWRRILAVWNLSLSLFSWIGAIRTAPQLYYNLTT 117
         :   .: :*. . ::  .     .   :  : . *  :     .:  .   *    :

Elo1  VMPCNHFNVND---------PPVANLLWLFYISKVWDFWDTIFIVLGKKWRQLSFLHVYH 149
Elo2  VMNRDHPFIGSRSLVGAALHSGSSYAVWVHYCDKYLEFFDTYFMVLRGKMDQVSFLHIYH 172
Elo3  YSLRDNLCDDPAALYGS---GSTGLWVQLFILSKFPELLDTFFIVIHKKP--LIFLHWYH 172
          ::   .             .  : :.  .*  :: ** *:*:  *   : *** **

Elo1  HTTIFLFYWLNANVLYDGDIFLTILLNGFIHTVMYTYYFICMHTKDPKTGKSLPIWWKSS 209
Elo2  HTTIAWAWWIALRFSPGGDIYFGALLNSIIHVLMYSYYALALLK--------VSCPWKRY 224
Elo3  HITVLLYCWHSYVTTSPSGLFF-VVMNYSVHAVMYGYYFLMAVKFRPKWFNPMFVTFMQL 231
      * *:    *        ..:::  ::*  :*.:** ** :   .       :   :

Elo1  LTAFQLLQFTIMMSQA-------TYLVFHGCDKVSLRITIVYFVY------ILSLFFLFA 256
Elo2  LTQAQLLQFTSVVVYTGCTGYTHYYHTKHGADETQPSLGTYYFCCGVQVFEMVSLFVLFS 284
Elo3  SQMFIGVGVTIVAFYYYS-----NPILGKTCHIRKENNVAAFVMYG-------SYFYLFA 279
            : .* :               : ..  .      :.          * * **:

Elo1  QFFVQSYMAPKKKKSA---------------------------------------------- 272
Elo2  IFYKRSYSKKNKSGGKDSKKNDDGNNEDQCHKAMKDISEGAKEVVGHAAKDAGKLVATAS 344
Elo3  QFFVARYYKVKVKGDAKKKKVV---------------------------------------- 301
       *:   *   : . .

Elo1  --------------
Elo2  KAVKRKGTRVTGAM 358
Elo3  --------------
```

Fig. 2 Alignment of amino acid sequences of elongases in this study. *Underlined* is the LHxYHH histidine-motif of Δ5 and Δ6 elongases. *Boxed sequences* for Elo 1 and 2 are the PUFA elongase motif, and the *boxed sequence* for Elo3 is a saturated/mono-unsaturated elongase motif

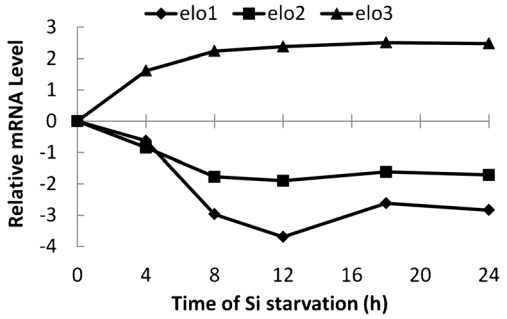

Fig. 3 mRNA level changes of the *elo* genes in response to Si starvation

(FAME) were extracted in 1 mL hexane and analyzed by GC-MS. C19 FAME was used to create a standard curve and served as an internal standard.

Results

Analysis of *T. pseudonana* FA elongase sequences

Previous data and our analysis indicated that the genome of *T. pseudonana* encodes 3 genes for FA elongases and 20 genes for FA desaturases (Armbrust et al. 2004; Tonon et al. 2005; Cook, unpublished data). All three elongases (Thaps3_3741=elo1, Thaps3_93=elo2, Thaps3_728=elo3) contained the Δ5/Δ6 motif LHxYHH (Fig. 2), which indicated that they catalyze the elongation of fatty acids with a double bond at position 5 or 6. However, none of the *T. pseudonana* elongases contained the Δ9 motif (LQxFHH). As shown by expression in yeast (Meyer et al. 2004), elo1 should have a stronger preference for Δ6 FAs while elo2 has a stronger preference for Δ5 FAs. Elo2 is a homolog to a Δ5 elongase isolated from *P. tricornutum* which was functionally characterized in yeast (Jiang et al. 2014). Elo1 and 2 also contained the motif of a PUFA elongase (Fig. 2). Elo3 has a MUFA/SFA motif (Fig. 2) which is specific to elongases that add a two-carbon unit to saturated and mono-unsaturated fatty acids (Hashimoto et al. 2008). We assign these elongases to the steps diagrammed in Fig. 1. Among the genes that encode for FA desaturases (Tonon et al. 2005) is one with high similarity to delta 4 desaturase and several genes that encode for delta-6, 8, 12-desaturases. The presence of delta 6-elongase and delta 6-desaturase genes, but not delta 9-elongase, indicates that the conversion of ALA to C20:4 occurs through the SDA (18:4n-3) intermediate and not through the alternative pathway involving the ETE (20:3n-3) intermediate in *T. pseudonana* (Fig. 1). Moreover, the conversion of EPA to DHA in *T. pseudonana* does not require the bypass path, which involves elongation to C24 chain and then a beta-oxidation step, since *T. pseudonana* contains genes that encode for delta4-desaturase which adds the sixth double bond to the 22:5 chain to make C22:6 (Fig. 1). The scheme depicted in Fig. 1 is consistent with previous functional analyses (Tonon et al. 2005) and the major pathway of EPA synthesis determined by isotope labeling in *P. tricornutum* (Aroa and Yamada 1994).

Transcript changes of the FA elongase genes of *T. pseudonana* and the predicted subcellular localization of their proteins

To understand more fully the possible roles of the three elongases, we monitored changes in their mRNA levels and

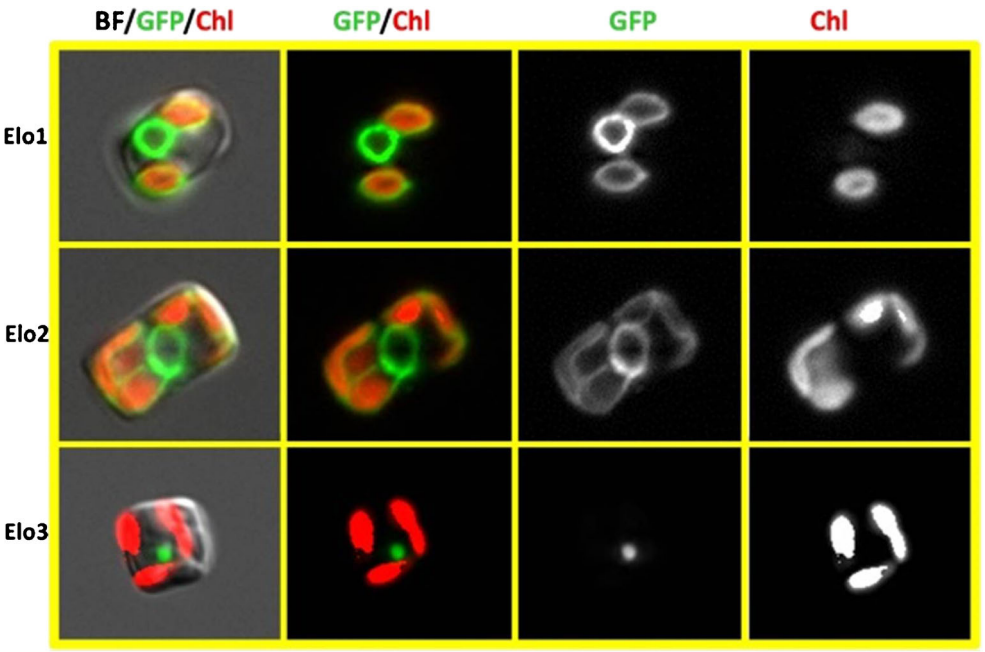

Fig. 4 Sub-cellular localization of fatty acid elongase proteins. *BF* bright field, *GFP* green fluorescent protein, *Chl* chlorophyll

determined their intracellular location. mRNA level changes were monitored during silicon starvation-induced lipid accumulation using whole genome microarrays (Smith et al. submitted). After placing cells into silicon-depleted medium, there is a general increase in FAs and particularly triacylglycerol (TAG) especially after 8 h (Smith et al. submitted). *Elo1* and *elo2* genes that encode for the Δ6 and Δ5 PUFA elongases, respectively, show decreased mRNA levels as a result of Si starvation while the S/MUFA elongase, *elo3*, increased (Fig. 3).

We examined the intracellular location of the elongases both bioinformatically and directly using GFP fusions. For bioinformatically predicted localization, we first verified the Thaps vers. 3 gene model using RNAseq data (Abbriano et al. unpublished), which supported the established gene models for all three elongases, also verifying the protein sequence shown in Fig. 2. None of the elo proteins contained a predicted mitochondrial targeting sequence. Using SignalP 3.0 (Bendtsen et al. 2004), Elo1 had a predicted signal anchor sequence, Elo2 had a predicted signal cleavage sequence (AFP-AA), and Elo3 had no prediction. Signal cleavage for Elo2 was also predicted using TargetP 1.1 (Emanuelsson et al. 2000), and a low confidence chloroplast targeting prediction was obtained using ChloroP1.1 (Emanuelsson et al. 1999).

To directly determine the intracellular location of each protein, we generated constructs in which the coding sequence of each *elo* gene was fused to GFP and placed under control of *fcp* 5′ and 3′ flanking sequences. Transformant lines were tested by PCR to verify they contained the appropriate construct. Examination of GFP fluorescence in transgenic lines indicated that Elo1 and Elo2 were localized in the ER membrane, which surrounds the nucleus and chloroplasts in diatoms (Fig. 4). Elo3 was localized in a small unidentified vesicle or organelle (Fig. 4). The same pattern of subcellular localization appeared throughout exponential into stationary phase of growth (data not shown).

Growth rate and maximal cell density of the elo transgenic lines

The transgenic lines used to determine localization also would serve to evaluate the effect of overexpression of these proteins. We also independently generated overexpression lines that lacked the GFP fusion. Several independent transgenic lines of each construct were tested for their growth rate and the maximal cell density. No significant difference was shown either in the growth rate or other tested parameters such as TAG accumulation or fatty acid profile between the non-fusion and the GFP-fusion lines. For each elongase, two or more GFP-fusion lines were compared to non-fusion lines. As shown in Fig. 5, most fcp-elo lines had a growth rate similar to wild type. Although some of the lines started with a lower inoculate (Fig. 5b elo1-GFP1 and elo3_GFP1), the slope of their growth rate was similar to wild type. Three lines with

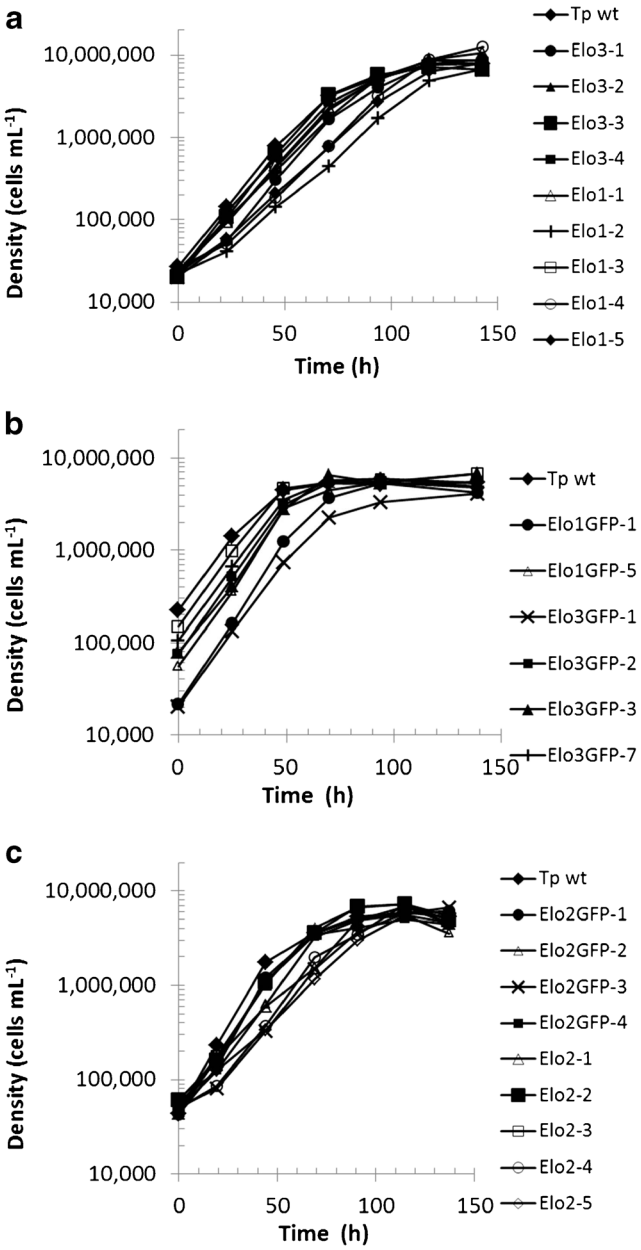

Fig. 5 Growth curves of transformant lines of the elongase genes. Different lines of *T. pseudonana* that contain an fcp-elongase construct as indicated were grown in ASW at 18 °C under constant light. **a** Lines with fcp-elo1 and fcp-elo3. **b** Lines with fcp-elo1GFP and fcp-elo3GFP. **c** Lines with fcp-elo2 and fcp-elo2GFP

fcp-elo1 and two lines with fcp-elo2 (Fig.5a, c) demonstrated slightly slower growth rate relative to wild type; however, since this phenotype did not occur in all the lines of a particular elongase, it might have been caused by the insertional position in the genome, which could disturb expression of another gene that affects growth. The maximum cell density to which all the fcp-elo transgenic lines reached was similar to that of the wild-type culture. Therefore, overexpression of each of the three *T. pseudonana* elongases did not substantially influence the growth of the cells.

Table 1 Fatty acid composition of wild type (wt) and overexpression lines (mg fatty acid•mg^{-1} dry weight)

FA formula	Exponential phase				Stationary phase				no Si			
	wt	Elo1	Elo2	Elo3	wt	Elo1	Elo2	Elo3	wt	Elo1	Elo2	Elo3
C14:0	0.013	0.013	0.015	0.012	0.020	0.023	0.026	0.022	0.016	0.020	0.018	0.019
C16:0	0.024	0.022	0.022	0.017	0.031	0.035	0.031	0.026	0.026	0.032	0.026	0.024
C16:1	0.019	0.021	0.019	0.018	0.035	0.034	0.031	0.029	0.040	0.049	0.038	0.041
C16:2	0.005	0.004	0.005	0.005	0.008	0.008	0.008	0.008	0.004	0.004	0.004	0.005
C16:3	0.008	0.007	0.008	0.007	0.012	0.011	0.013	0.013	0.008	0.009	0.007	0.009
C16:4	0.000	0.000	0.000	0.001	0.001	0.001	0.001	0.001	0.001	0.001	0.000	0.000
C18:0	0.000	0.001	0.000	0.000	0.000	0.000	0.000	0.000	0.000	0.000	0.000	0.000
C18:1	0.001	0.000	0.000	0.000	0.001	0.001	0.001	0.001	0.000	0.000	0.000	0.000
C18:2	0.000	0.000	0.000	0.000	0.000	0.000	0.000	0.000	0.000	0.000	0.000	0.000
C18:3	0.000	0.000	0.000	0.000	0.000	0.000	0.000	0.000	0.000	0.000	0.000	0.000
C18:4	0.006	0.004	0.007	0.004	0.012	0.009	0.014	0.011	0.008	0.007	0.009	0.008
C20:5	0.010	0.012	0.009	0.011	0.016	0.018	0.010	0.016	0.016	0.018	0.016	0.019
C22:6	0.001	0.001	0.003	0.002	0.003	0.002	0.003	0.002	0.002	0.004	0.005	0.003
Total	0.085	0.086	0.088	0.077	0.138	0.142	0.138	0.130	0.123	0.145	0.124	0.128

Neutral lipid accumulation in the elo transgenic lines

We tested whether the accumulation of neutral lipids as TAG was affected in the transgenic *fcp-elo* lines during growth and under Si starvation by monitoring BODIPY or Nile Red fluorescence (Trentacoste et al. 2013). Cultures were grown in continuous light conditions and samples were taken for analysis at certain time points during growth and after 24 h of Si starvation. Although some tendencies were observed, there were no statistically significant differences in the transgenic lines compared with wild type (data not shown). This suggests that the modifications have no direct effect on TAG accumulation.

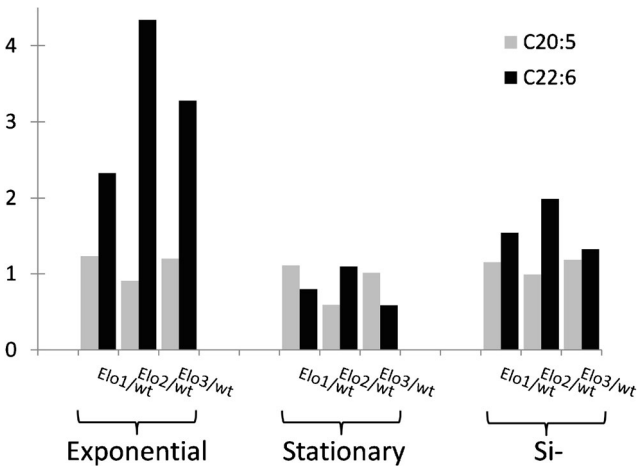

Fig. 6 The ratio of EPA and DHA in transgenic lines relative to wild type under three different growth conditions

Analyzing the lipid profile of elongase overexpressing lines

We next examined whether overexpression of a specific elongase affected the cellular fatty acid composition. Independent transgenic lines; three elo1 lines, four elo2 lines, and five elo3 lines were tested. Cells were collected during exponential phase, stationary phase, and at 24 h of Si starvation, for a lipid profile analysis. The abundance of most FA components did not change relative to wild type under the various growth conditions (Table 1). Comparing the relative abundance of EPA and DHA in the transgenic lines relative to wild type (Fig. 6) indicated generally little change in EPA with a possible exception of Elo2 overexpression in stationary phase, where EPA was reduced. In contrast, DHA was substantially increased, by 2.3–4.3-fold, relative to wild type in all three transgenic manipulations during exponential growth (Fig. 6). Levels were equal to or slightly lower than wild type in stationary phase, and slightly higher, particularly with the Elo2 overexpression lines, under silicon starvation.

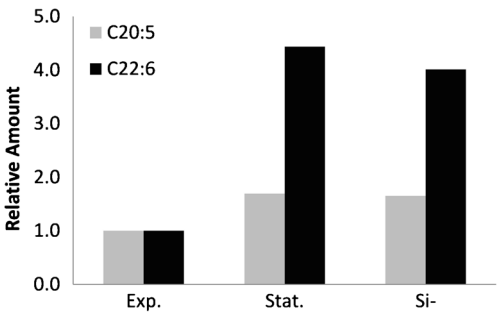

Fig. 7 Relative amount of EPA (C20:5) and DHA (C22:6) in wild-type *T. pseudonana* in stationary phase and silicon starvation, relative to exponential growth

Discussion

Our analysis identified three elongase steps involved in LCPUFA synthesis, and sequence analysis (Fig. 2) coupled with previous work (Meyer et al. 2004; Jiang et al. 2014), enabled determination of the steps they catalyzed. Additional analysis of desaturases showed that alternative pathways were not present in *T. pseudonana* (Tonon et al. 2005; Fig. 1), as has been surmised in *P. tricornutum* (Aroa and Yamada 1994). Continuing clarification of these pathways will facilitate metabolic engineering efforts (Domergue et al. 2002; 2003; Peng et al. 2014).

During silicon starvation in diatoms, TAG accumulation is induced (Roessler 1988; Yu et al. 2009). In a 24-h time course of silicon starvation in *T. pseudonana*, FAs begin to increase by 4 h, and TAG starts to substantially increase between 8 and 12 h (Smith et al., submitted). Examination of mRNA expression data shows that *elo3* is specifically induced by 4 h (Fig. 3). This enzyme catalyzes an early step in the pathway, converting C16:0 to C18:0 (Fig. 1), and induction of its mRNA is consistent with increased carbon flux into LCPUFA synthesis, even though C18 compounds do not accumulate. The delta 6 desaturase has been considered a rate-limiting step for the pathway in higher plants; however, lack of accumulation of substantial amounts of C18:3, 18:2, or 18:1 are inconsistent with that in *T. pseudonana* (Table 1). mRNA for *elo1* and *elo2* are substantially downregulated during silicon starvation (Fig. 3), consistent with a decrease in carbon flux through these steps. However, in wild-type lines, we document a slight increase in EPA and a substantial increase (4–4.5-fold) in DHA after 24 h of silicon starvation (Fig. 7), suggesting that any possible decreases in enzymes involved in the later steps of LCPUFA synthesis is offset by increased carbon flux into the pathway. Although not a true flux analysis, the data are consistent with the major rate limitation occurring at the early steps in the pathway.

To our knowledge FA elongases have not been previously localized in diatoms. In our analysis, Elo1 and 2 are localized in the ER (Fig. 4). A delta 6 elongase has been localized to the ER in the green alga *Myrmecia incisa* (Yu et al. 2012). In *T. pseudonana*, the SFA elongase, Elo3, is localized to an unidentified intracellular organelle or vesicle (Fig. 4). Overall, the localization data support that LCPUFA synthesis occurs in association with the ER in *T. pseudonana*, but precursors into this pathway are synthesized in an unidentified organelle.

Regardless of which elongase was overexpressed, DHA levels showed the greatest resulting increase (Table 1, Fig. 6). Elo2 overexpression always resulted in higher DHA than Elo1 or 3 overexpression (Table 1, Fig. 6), consistent with higher flux through the C20:5 to C22:5 step (Fig. 1). The increase in DHA was most substantial under exponential growth conditions (Table 1, Fig. 6), which would be when carbon flux into FA storage forms would be minimal compared with stationary phase or Si starvation. Previous work in *P. tricornutum*, in which a heterologous delta 5 elongase from *Ostreococcus tauri* was overexpressed, indicated 2-fold less EPA during exponential growth and 2.1-fold less in stationary phase (Hamilton et al. 2014). DHA increased 3.7-fold in exponential phase and 8-fold in stationary phase. Our Elo2 (delta 5 elongase) overexpression showed 1.1-fold less EPA in exponential phase, 1.5-fold less in stationary, and 1.04-fold more in Si- (Fig. 6). DHA was increased by 3.76-fold in exponential phase, 1.74-fold in stationary, and 2.75-fold in Si- (Fig. 6). Differences between the two studies could be due to the use of native or heterologous enzymes or a fundamental difference in regulation of carbon flux in the pathway in these two diatom species.

Overall, our results indicate that engineering of the elongase steps in the pathway has a small effect under silicon starvation conditions when the total amount of EPA and DHA per cell are maximal, resulting in a significant increase only in DHA. This can be useful; under exponential growth, the wild-type EPA/DHA ratio is 16:1, which changes to approximately 6:1 under stationary phase and during silicon starvation. In the Elo2 overexpression lines, the ratio drops to 3.2:1 under silicon starvation. The increased accumulation of DHA relative to EPA regardless of which elongase is overexpressed, as well as under silicon limitation, is consistent with preferential accumulation of the end product of the pathway. Other manipulations and combined manipulations could improve carbon flux into EPA and DHA synthesis or alter the ratio of EPA to DHA, for example, overexpression of a delta 5 desaturase in *P. tricornutum* resulted in increased neutral lipid and EPA (Peng et al. 2014).

Acknowledgments The authors are thankful to Joris Beld for helpful advice about the FAME reaction experiments and technical guidance and support with GC-MS experiments, to Sarah Smith for sharing unpublished gene expression data and helpful discussions, and to Raffaela Abbriano for sharing unpublished RNAseq data and helpful advice and discussions of various experiments in this work.

Funding This research was supported by Air Force Office of Scientific Research (AFOSR) grants FA9550-08-1-0178, US Department of Energy grants DE-EE0001222 and DE-EE0003373, National Science Foundation grant CBET-0903712, and California Energy Commission's "California Initiative for Large Molecule Sustainable Fuels," agreement number 500-10-039.

Conflict of interest The authors declare that they have no competing interests.

References

Armbrust EV, Berges JA, Bowler C, Green BR, Martinez D, Putnam NH et al (2004) The genome of the diatom *Thalassiosira pseudonana*: ecology, evolution, and metabolism. Science 309:79–86

Aroa T, Yamada M (1994) Biosynthesis of polyunsaturated fatty acids in the marine diatom *Phaeodactylum tricornutum*. Phytochemistry 35: 1177–1181

Atalah E, Hernández Cruza CM, Izquierdo MS, Rosenlund G, Caballero MJ, Valencia A, Robaina L (2007) Two microalgae *Crypthecodinium cohnii* and *Phaeodactylum tricornutum* as alternative source of essential fatty acids in starter feeds for seabream (*Sparus aurata*). Aquaculture 270:178–185

Bendtsen JD, Nielsen H, von Heijne G, Brunak S (2004) Improved prediction of signal peptides: signalP 3.0. J Mol Biol 340:783–795

Bernardi R, de Souza R, Escobar J, Ferreira CF, Silveira PP (2012) Fetal and neonatal levels of omega-3: effects on neurodevelopment, nutrition, and growth. Sci World J 2012:202473

Brenna JT, Salem N Jr, Sinclair AJ, Cunnane SC (2009) Alpha-linolenic acid supplementation and conversion to n-3 long-chain polyunsaturated fatty acids in humans. Prostaglandins Leukot Essent Fat Acids 80:85–91

Cunnane SC, Menard CR, Likhodii SS, Brenna JT, Crawford MA (1999) Carbon recycling into de novo lipogenesis is a major pathway in neonatal metabolism of linoleate and alpha-linolenate Prostag. Prostaglandins Leukot Essent Fat Acids 60:387–392

Darley WM, Volcani BE (1969) Role of silicon in diatom metabolism: a silicon requirement for deoxyribonucleic acid synthesis in the diatom *Cylindrotheca fusiformis* reimann and Lewin. Exp Cell Res 58: 334–342

Domergue F, Lerchl J, Zahringer U, Heinz E (2002) Cloning and functional characterization of *Phaeodactylum tricornutum* front-end desaturases involved in eicosapentaenoic acid biosynthesis. Eur J Biochem 269:4105–4113

Domergue F, Spiekermann P, Lerchl J, Beckmann C, Kilian O, Kroth PG, Boland W, Zahringer U, Heinz E (2003) New insight into *Phaeodactylum tricornutum* fatty acid metabolism cloning and functional characterization of plastidial and microsomal 12-fatty acid desaturases. Plant Physiol 131:1648–1660

Dunahay TG, Jarvis EE, Roessler PG (1995) Genetic transformation of the diatoms *Cyclotella cryptica* and *Navicula saprophila*. J Phycol 31:1004–1012

Emanuelsson O, Nielsen H, von Heijne G (1999) ChloroP, a neural network-based method for predicting chloroplast transit peptides and their cleavage sites. Protein Sci 8:978–84

Emanuelsson O, Nielsen H, Brunak S, von Heijne G (2000) Predicting subcellular localization of proteins based on their N-terminal amino acid sequence. J Mol Biol 300:1005–1016

Gamoh S, Hashimoto M, Sugioka K, Hossain MS, Hata N, Misawa Y, Masumura S (1999) Chronic administration of docosahexaenoic acid improves reference memory-related learning ability in young rats. Neurosciences 93:237–241

Grima EM, Medina AR, Gimenez AG, Gonzalez MJI (1996) Gram-scale purification of eicosapentaenoic acid (EPA, 20:5n-3) from wet *Phaeodactylum tricornutum* UTEX 640 biomass. J Appl Phycol 8: 359–367

Hamilton ML, Haslam RP, Napier JA, Sayanova O (2014) Metabolic engineering of *Phaeodactylum tricornutum* for the enhanced accumulation of omega-3 long chain polyunsaturated fatty acids. Metab Eng 22:3–9

Harel M, Koven W, Lein I, Barb Y, Behrens P, Stubblefield J, Zohar Y, Place AR (2002) Advanced DHA, EPA and ArA enrichment materials for marine aquaculture using single cell heterotrophs. Aquaculture 213:347–362

Hashimoto M, Hossain S, Shimada T, Sugioka K, Yamasaki H, Fujii Y, Ishibashi Y, Oka JI, Shido O (2002) Docosahexaenoic acid provides protection from impairment of learning ability in Alzheimer's disease model rats. J Neurochem 81:1084–1091

Hashimoto K, Yoshizawa AC, Okuda S, Kuma K, Goto S, Kanehisa M (2008) The repertoire of desaturases and elongases reveals fatty acid variations in 56 eukaryotic genomes. J Lipid Res 49:183–191

Jiang M, Guo B, Wan X, Gong YM, Zhang YB, Hu CJ (2014) Isolation and characterization of the diatom *Phaeodactylum* delta 5-elongase gene for transgenic LC-PUFA production in *Pichia pastoris*. Mar Drugs 12:1317–1334

Khozin-Goldberg I, Iskandarov U, Cohen Z (2011) LC-PUFA from photosynthetic microalgae: occurrence, biosynthesis, and prospects in biotechnology. Appl Microbiol Biotech 91:905–915

Kitessa SM, Abeywardena M, Wijesundera C, Nichols PD (2014) DHA-containing oilseed: a timely solution for the sustainability issues surrounding fish oil sources of the health-benefitting long-chain omega-3 oils. Nutrients 6:2035–2058

Leyton J, Drury PJ, Crawford M (1987) Differential oxidation of saturated and unsaturated fatty acids in vivo in the rat. Brit J Nut 57: 383–93

Li M, Ou X, Yang X, Guo D, Qian X, Xing L, Li M (2011) Isolation of a novel C18-Δ9 polyunsaturated fatty acid specific elongase gene from DHA-producing Isochrysis galbana H29 and its use for the reconstitution of the alternative Δ8 pathway in *Saccharomyces cerevisiae*. Biotechnol Lett 33:1823–1830

Meyer A, Kirsch H, Domergue F, Abbadi A, Sperling P, Bauer J, Cirpus P, Zank TK, Moreau H, Roscoe TJ (2004) More novel fatty acid elongases and their use for the reconstitution of docosahexaenoic acid biosynthesis. J Lipid Res 45:1899–1909

Molloy C, Doyle LW, Makrides M, Anderson PJ (2012) Docosahexaenoic acid and visual functioning in preterm infants: a review. Neuropsych Rev 22:425–37

Peng KT, Zheng CN, Xue J, Chen XY, Yang WD, Liu JS, Bai WB (2014) Li HY Delta 5 fatty acid desaturase upregulates the synthesis of polyunsaturated fatty acids in the marine diatom *Phaeodactylum tricornutum*. J Agric Food Chem 62:8773–8776

Poulsen N, Chesley PM, Kroger N (2006) Molecular genetic manipulation of the diatom *Thalassiosira pseudonana* (Bacillariophyceae). J Phycol 42:1059–1065

Qi B, Beaudoin F, Fraser T, Stobart AK, Napier JA, Lazarus CM (2002) Identification of a cDNA encoding a novel C18- Δ9 polyunsaturated fatty acid-specific elongating activity from the docosahexaenoic acid. FEBS Lett 510:159–165

Roessler PG (1988) Effects of silicon deficiency on lipid composition and metabolism in the diatom *Cyclotella cryptica*. J Phycol 24:394–400

Ruxton CHS, Reed SC, SimpsonMJA MKJ (2004) The health benefits of omega-3 polyunsaturated fatty acids: a review of the evidence. J Human Nutr Diet 17:449–459

Shrestha RP, Hildebrand M (2015) Evidence for a regulatory role of diatom silicon transporters in cellular silicon responses. Euk Cell 14:29–40

Simopoulos AP (2008) The importance of the omega-6/omega-3 fatty acid ratio in cardiovascular disease and other chronic diseases. Exp Biol Med 233:674–88

Sinn N, Milte C, Howe PRC (2010) Oiling the brain: a review of randomized controlled trials of omega-3 fatty acids in psychopathology across the lifespan. Nutrients 2:128–70

Soederberg M, Edlund E, Kristensson K, Dallner G (1991) Fatty acid composition of brain phospholipids in aging and in Alzheimer's disease. Lipid 26:421–425

Tonon T, Harvey D, Larson TR, Graham IA (2002) Long chain polyunsaturated fatty acid production and partitioning to triacylglycerols in four microalgae. Phytochemistry 61:15–24

Tonon T, Harvey D, Qing R, Li Y, Larson TR, Graham IA (2004) Identification of a fatty acid Δ11-desaturase from the microalga *Thalassiosira pseudonana*. FEBS Lett 563:28–34

Tonon T, Sayanova O, Michaelson LV, Qing R, Harvey D, Larson TR, Li Y, Napier JA, Graham IA (2005) Fatty acid desaturases from the microalga *Thalassiosira pseudonana*. FEBS J 272:3401–3412

Trentacoste EM, Shrestha R, Smith SR, Glé C, Hartmann AC, Hildebrand M, Gerwick WH (2013) Metabolic engineering of lipid catabolism increases microalgal lipid accumulation without compromising growth. Proc Natl Acad Sci U S A 110:19748–19753

Turchini GM, Nichols PD, Barrow C, Sinclair AJ (2012) Jumping on the omega-3 bandwagon: distinguishing the role of long-chain and short-chain omega-3 fatty acids. Crit Rev Food Sci Nutr 52:795–803

Venegas-Calerón M, Sayanova O, Napie J (2010) An alternative to fish oils: Metabolic engineering of oil-seed crops to produce omega-3 long chain polyunsaturated fatty acids. Prog Lipid Res 49:108–19

Vermunt SH, Mensink RP, Simonis MM, Hornstra G (2000) Effects of dietary alpha-linolenic acid on the conversion and oxidation of ^{13}C-alpha-linolenic acid. Lipids 35:137–42

Volkman JK, Jeffrey SW, Nichols PD, Rogers GI, Garlan CD (1989) Fatty acid and lipid composition of 10 species of microalgae used in mariculture. J Exp Mar Biol Ecol 128:219–240

Voss A, Reinhart M, Sankarappa S, Sprecher H (1991) The metabolism of 7,10,13,16,19-docosapentaenoic acid to 4,7,10,13,16,19-docosahexaneoic acid in rat liver is independent of a 4-desaturase. J Biol Chem 266:19995–20000

Wallis JG, Browse J (1999) The Δ8-desaturase of *Euglena gracilis*: an alternate pathway for synthesis of 20-carbon polyunsaturated fatty acids. Arch Biochem Biophys 365:307–316

Wallis JG, Watts JL, Browse J (2002) Polyunsaturated fatty acid synthesis: what will they think of next? Trends Biol Sci 27:467–473

Yu ET, Zendejas FJ, Lane PD, Gaucher S, Simmons BA, Lane TW (2009) Triacylglycerol accumulation and profiling in the model diatoms *Thalassiosira pseudonana* and *Phaeodactylum tricornutum* (Bacillariophyceae) during starvation. J Phycol 21:669–681

Yu SY, Li H, Tong M, Ouyang LL, Zhou ZG (2012) Identification of a Δ6 fatty acid elongase gene for arachidonic acid biosynthesis localized to the endoplasmic reticulum in the green microalga *Myrmecia incisa* Reisig. Gene 493:219–227